Efficiency of photoprotection in microphytobenthos: role of vertical migration and the xanthophyll cycle against photoinhibition

Joao Serôdio, Joao Ezequiel, Alexandre Barnett, Jean-Luc Mouget, Vona Méléder, Martin Laviale, Johann Lavaud

Efficiency of photoprotection in microphytobenthos: the role of vertical migration and the xanthophyll cycle against photoinhibition

João Serôdio[1,2*], João Ezequiel[1], Alexandre Barnett[2], Jean-Luc Mouget[3], Vona Méléder[2,4], Martin Laviale[1,4], Johann Lavaud[2]

[1] Departamento de Biologia and CESAM – Centro de Estudos do Ambiente e do Mar, Universidade de Aveiro, Campus de Santiago, 3810-193 Aveiro, Portugal

[2] UMR 7266 'LIENSs', CNRS-University of La Rochelle, Institute for Coastal and Environmental Research (ILE), 2 rue Olympe de Gouges, 17 000 La Rochelle, France

[3] Mer Molécules Santé – MMS EA 2160, Université du Maine. Av. O. Messiaen, 72085 Le Mans Cedex 9, France

[4] Mer Molécules Santé – MMS EA 2160, Université de Nantes. BP 92 208, 44322, Nantes Cedex 3, France

* Corresponding author: jserodio@ua.pt

Abstract

The capacity of estuarine microphytobenthos to withstand the variable and extreme conditions of the intertidal environment, prone to cause photoinhibition of the photosynthetic apparatus, has been attributed to particularly efficient photoprotection mechanisms. However, little is known regarding its actual photoprotection capacity or the mechanisms responsible for the protecting against photoinhibition. This study addressed these questions by (i) quantifying the photoprotection capacity and the extent of photoinhibition under high light exposure, (ii) estimating the contribution of vertical migration and the xanthophyll cycle to overall photoprotection and (iii) evaluating the effects of photoacclimation state. A new experimental protocol was developed, combining (i) chlorophyll fluorescence imaging, for the simultaneous measurement of replicates and experimental treatments, (ii) specific inhibitors for vertical migration and for the xanthophyll cycle, to quantify the relative contribution of each process, and (iii) recovery kinetics analysis of photosynthetic activity during light stress-recovery experiments, to distinguish reversible downregulation from photoinhibition. The results showed a high photoprotective capacity in both studied periods, May and October, with photoinhibition rates remaining below 20%. A clear change in photoacclimation state was obeserved, following the seasonal change in solar radiation, with acclimation to lower irradiances in autumn being associated with higher susceptibility to photoinhibition. Also the relative importance of vertical migration and the xanthophyll cycle varied between the sampling periods. While the two processes displayed a similar role in spring/summer, vertical migration became the dominant photoprotective process in autumn. However, the contribution of the two processes to overall photoprotection

reached only ca. 20%, suggesting the participation of other photoprotective mechanisms.

Running head: Photoprotection and photoinhibition in microphytobenthos

Key index words: microphytobenthos; photoinhibition; photoprotection; xanthophyll cycle; vertical migration; non-photochemical quenching; chlorophyll fluorescence; diatoms

INTRODUCTION

Benthic microalgae inhibiting estuarine intertidal flats are exposed to extreme and highly variable environmental conditions. Particularly during low tide, the sedimentary environment is characterized by the exposure to high levels of solar irradiance (Serôdio & Catarino 1999), including UV radiation (Waring et al. 2007, Mouget et al. 2008), extreme temperatures and salinities (Brotas et al. 2003, Rijstenbil 2005), intense rates of desiccation (Coelho et al. 2009), supersaturated oxygen concentrations (Chevalier et al. 2010), and nutrient and carbon depletion (Miles & Sundbäck 2000, Cook & Røy 2006). Being potentially damaging to the photosynthetic apparatus when acting individually, the combined effects of all these factors likely concur to the photoinhibition of photosynthesis of microphytobenthos microalgae. Of particular importance is the exposure to direct sunlight, which can result in excessive reductant pressure and in the formation of intracellular reactive oxygen species (ROS; Roncarati et al. 2008, Waring et al. 2010). High levels of ROS cause the permanent inactivation of photosystem II (PSII) protein D1, negatively impacting on photosynthetic yield and on primary productivity (Nishiyama et al. 2006).

Despite these harsh conditions, microphytobenthos of intertidal flats typically exhibit high growth rates, forming dense and diverse sedimentary biofilms, and are recognized as a major contributor to ecosystem-level carbon fixation and primary productivity (Underwood & Kromkamp 1999). Furthermore, the apparent lack of photoinhibition in microphytobenthic biofilms has been repeatedly reported (Kromkamp et al. 1998, Underwood 2002, Blanchard & Cariou-LeGall 1994, Blanchard et al. 2004, Underwood et al. 2005, Van Leeuwe et al. 2008). This success in coping with high light stress may be explained by the combined operation of two processes, the xanthophyll cycle and vertical migration, which could result in an overall particularly

efficient photoprotection (Serôdio et al. 2008, Perkins et al. 2010). In diatoms, the group of microalgae that typically dominate in microphytobenthos assemblages, the xanthophyll cycle has been reported to provide an exceptionally high photoprotective capacity (Lavaud 2007, Brunet & Lavaud 2010, Goss & Jakob 2010). This is particularly true for microphytobenthos *in situ* (Serôdio et al. 2005, Van Leuwee et al. 2008, Jordan et al. 2010, Chevalier et al. 2010). To this also seems to contribute the activation of the xanthophyll cycle in the dark, attributed to cholorespiratory activity, which has been considered as potentially advantageous during prolonged periods of darkness (Jakob et al. 2001, Cruz et al. 2011), a situation common in the sedimentary environment.

On the other hand, the negative phototactic behavior of benthic diatoms, mostly raphid pennates, under high light has long been interpreted as a form of avoidance of excessive light levels that would otherwise cause photoinhibition (Admiraal 1984, Underwood & Kromkamp 1999, Consalvey et al. 2004, Waring et al. 2007).

This subject has attracted substantial attention in recent years, particularly centered on the effects of vertical migration on biofilm photophysiology (Consalvey et al. 2004, Jesus et al. 2006, Waring et al. 2007, Mouget et al. 2008, Perkins et al. 2010, Cartaxana et al. 2011), and became facilitated by the introduction of a diatom motility inhibitor (Cartaxana et al. 2008). However, these studies have been focused on the response of photosynthetic activity during (Waring et al. 2007, Perkins et al. 2010) or shortly after light stress (Mouget et al. 2008), mostly through *in vivo* measurements of electron transport rate of PSII (ETR) or non-photochemical quenching (NPQ) of chlorophyll fluorescence (PAM fluorometry, see below; Table 1) (Perkins et al. 2011). Perhaps surprisingly, none of these studies has actually evaluated the efficiency of the photoprotection provided by these two processes or compared their role against

photoinhibition in microphytobenthos biofilms. The distinction between photoprotection and photoinhibition processes from chlorophyll fluorescence cannot be inferred from the decrease in ETR or formation of NPQ under high light, but requires the analysis of the recovery kinetics of photosynthetic activity following exposure to high light stress (Horton & Hague 1988, Walters & Horton 1991, Müller et al. 2001). In diatoms, a rapid (within minutes) component of this recovery can be attributed to the reversal of the xanthophyll cycle (q_E, or 'energy-dependent quenching') while photoinhibitory effects (q_I, or 'photoinhibitory quenching') can be quantified from a second, much slower (within hours) component (Müller et al. 2001, Lavaud 2007). The q_T (state-transition related quenching) component of NPQ recovery, which shows intermediate relaxation kinetics, does not exist in diatoms (Owens, 1986). As such, questions like 'How efficient are photoprotective processes in preventing photoinhibition in microphytobenthos biofilms?', 'What is the relative contribution of migration and the xanthophyll cycle for overall photoprotection?' or 'To what extent does photoinhibition occur in microphytobenthos?' are mostly unanswered.

This study was set out to address these questions, for which a new experimental protocol was designed, based on the combination of (i) chlorophyll fluorescence imaging, to allow the simultaneous measurement of a large number of samples and experimental treatments, (ii) the use of specific inhibitors for vertical migration and for the xanthophyll cycle, to quantify the relative contribution of each process to overall photoprotection, and (iii) the analysis of the recovery kinetics of photosynthetic activity following light stress, to distinguish downregulation due to the xanthophyll cycle and photoinhibition. This approach was further used to test the influence of photoacclimation state on photoprotection capacity and susceptibility to photoinhibition in microphytobenthic biofilms inhabiting a temperate intertidal mudflat.

MATERIALS AND METHODS

Sampling and sample preparation. Sediment samples were collected in the upper zone of an intertidal mudflat in the Baie de l'Aiguillon (46º15'18" N, 01º08'33" W), France, in late spring (May) and autumn (October) 2010, expected to show contrasting photoacclimation states following the seasonal variation in solar radiation (see below). The sampling site is composed of fine muddy sediments (< 63 µm) where microphytobenthic biofilms are largely dominated by diatoms (Herlory et al. 2004). During low tide, samples of the surface layers of sediment (approximately the top 1 cm) were collected using a spatula. In the laboratory, the sediment was sieved through a 500-µm mesh, to remove the mud snails *Hydrobia* sp. and other meio- and macrofauna, and was thoroughly mixed and spread in 4 cm deep plastic trays. The sediment was covered by water collected in the sampling site and left undisturbed overnight. In the next morning, at the start of the photoperiod, the slurries were again homogenized and identical portions of the resulting slurry were transferred to 24-well plates using a small spatula, filling the wells completely (ca. 3 ml). The well plates were exposed to homogeneous light field provided by two LED panels (equal contribution of red, far-red, blue and white LEDs; FloraLEDs panels, Plant Climatics, Germany) delivering a constant irradiance of 70 µmol quanta m^{-2} s^{-1} at the sample surface, in order to induce the upward migration of microalgae and the formation of the biofilm. Daily global solar radiation were obtained from a Meteo-France weather station located approximately 9 kms southwest from the sampling site, for two-week periods preceding the sampling dates, 15-30 May and 5-20 Octorber 2010.

Fluorescence measurements. Chlorophyll fluorescence was measured using an imaging-PAM fluorometer (Maxi-PAM M-series, Walz GmbH, Effeltrich, Germany).

158 The measuring area of the fluorometer covered each entire well plate, so that up to a
159 total of 24 sediment samples could be monitored simultaneously. All experiments were
160 carried out after biofilm formation. This was determined by measuring the fluorescence
161 level F_s, taken as a proxy for surface microalgal biomass, in a replicated set of samples
162 exposed to constant low light of 55 µmol quanta m^{-2} s^{-1}. Experiments were started after
163 F_s reached a plateau following the initial rise after on the onset of the light period which
164 typically took 2-3 hours of low light exposure. For each sample, the fluorescence signal
165 was calculated by averaging the values of all pixels included in an area of ca. 63.6 mm^2
166 (area of interest), which corresponded to ca. 1500 pixels, centered inside each well. This
167 area is smaller than the total area of each well (95.0 mm^2), the difference being due to
168 the exclusion of the edge of each sample, often not representative of the rest of the
169 biofilm. To minimize sample heating during prolonged exposure to high light, the
170 experiments were carried out in a temperature-controlled room, at 20 ºC, and the
171 fluorometer Perspex hood was maintained open at all times.
172 **Photoacclimation: light-response curves.** The photoacclimation state of the
173 samples was characterized by measuring light-response curves of ETR and of NPQ in
174 the two sampling periods. Light-response curves were generated by sequentially
175 exposing the samples to 7 levels of actinic light, up to 700 µmol quanta m^{-2} s^{-1}. Samples
176 were exposed to each light level for 3 min (a period previously confirmed allowing for
177 reaching a steady-state), after which a saturation pulse was applied and fluorescence
178 levels F_s and F_m' were recorded. Six replicated measurements (on six different wells)
179 were made for each light level. For each irradiance level, *E*, the relative ETR was
180 calculated from the product of *E* and the PSII effective quantum yield, $\Delta F/F_m'$ (Genty et
181 al. 1989):
182

$$\mathrm{ETR} = E \frac{F_m' - F_s}{F_m'} \quad (1)$$

ETR vs *E* curves were quantitatively described by fitting the model of Eilers & Peeters (1988), and by estimating the parameters α (the initial slope of the curve), $\mathrm{ETR_m}$ (maximum ETR) and E_k (the light-saturation, or photoacclimation, parameter):

$$\mathrm{ETR}(E) = \frac{E}{a E^2 + b E + c} \quad (2)$$

where

$$\alpha = \frac{1}{c}, \ \mathrm{ETR_m} = \frac{1}{b + \sqrt{ac}} \text{ and } E_k = \frac{c}{b + \sqrt{ac}} \quad (3)$$

Due to the unavoidable confounding effects of vertical migration on the measurement of F_m, NPQ was calculated using the adapted index, based on the relative difference between the maximum fluorescence measured during the construction of the light curve, $F_m'_m$, and upon exposure to light, F_m' (Serôdio et al. 2005):

$$\mathrm{NPQ} = \frac{F_{m,m}' - F_m'}{F_m'} \quad (4)$$

NPQ vs *E* curves were described by fitting the model of Serôdio & Lavaud (2011), and by estimating the parameters $\mathrm{NPQ_m}$ (maximum NPQ), E_{50} (irradiance corresponding to half of $\mathrm{NPQ_m}$) and *n* (sigmoidicity parameter):

$$\mathrm{NPQ}\ (E) = \mathrm{NPQ}_{m} \frac{E^{n}}{E_{50}^{n} + E^{n}} \quad (5)$$

These models were fitted using a procedure written in MS Visual Basic and based on MS Excel Solver. Model parameters were estimated iteratively by minimizing a least-squares function, forward differencing, and the default quasi-Newton search method. The model was fitted to individual light-response curves. Estimates of model parameters were compared using the Student's *t*-test. The standard errors of the parameter estimates were calculated following Ritchie (2008).

Photoprotection vs photoinhibition: light stress-recovery experiments. The photoprotection capacity of microphytobenthos biofilms was estimated by quantifying the recovery of $\Delta F/F_m'$ following a prolonged exposure to supersaturating irradiance. Three replicates were sequentially exposed to: (i) low light level of 55 μmol quanta m^{-2} s^{-1}, for a minimum of 15 min, to ensure full light-activation of the photosynthetic apparatus and to determine pre-stress reference levels of $\Delta F/F_m'$; (ii) supersaturating light level of 1200 μmol quanta m^{-2} s^{-1} for 3 hrs, to potentially induce photoinhibitory effects; (iii) low light (55 μmol quanta m^{-2} s^{-1}) for a minimum of 15 min to record the recovery kinetics. During the whole experiment, $\Delta F/F_m'$ was measured by applying saturating pulses every 90 s. The recovery of $\Delta F/F_m'$ upon the return to low light conditions was described by fitting an exponential function, adapted from a first-order kinetics model derived for describing the kinetics of NPQ (Olaizola & Yamamoto 1994, Serôdio et al. 2005):

$$\Delta F / F_{m}'(t) = \Delta F / F_{m,rec}' + \left[\Delta F / F_{m}'(0) - \Delta F / F_{m,rec}'\right] e^{-kt} \quad (6)$$

where t is the time during recovery, $\Delta F/F_m'(0)$ and $\Delta F/F_{m',rec}$ represent the PSII quantum yield levels at the start of the recovery period and after full recovery (associated to q_E), and k is the rate constant of $\Delta F/F_m'$ recovery. The values of $\Delta F/F_m'$ estimated by the model for t = 10.5 min, expressed as a percentage of the pre-stress levels, were used for estimating the effective photoprotective capacity of the biofilm. The remaining relative difference between pre- and post-stress levels of $\Delta F/F_m'$ was used as an estimate of the photoinhibitory effects imposed by high light.

The photoprotective roles of vertical migration and of the xanthophyll cycle were studied by applying specific inhibitors of the two processes. Vertical migration was inhibited by the diatom motility inhibitor Latrunculin (Lat) A, shown to effectively inhibit cell motility without causing appreciable effects on the photosynthetic activity (Cartaxana et al. 2008). To inhibit the activity of the xanthophyll cycle, the inhibitor of the diadinoxanthin de-epoxidase (DDE) dithiothreitol (DTT) was used. DTT is commonly used to inhibit the conversion of the pigment diadinoxanthin (DD) into the photoprotective form diatoxanthin (DT) (Lavaud et al. 2002a). DTT was applied in combination with Lat A, in order to ensure that the cells having the xanthophyll cycle inhibited remained exposed to high light.

The contribution of vertical migration to overall photoprotection capacity of the biofilm was estimated by the difference between the levels of $\Delta F/F_m'$ recovery in control (free moving cells) and Lat A-treated (vertical migration inhibited) samples. The contribution of the xanthophyll cycle was estimated by comparing the levels of $\Delta F/F_m'$ recovery in the samples treated with Lat A (only vertical migration inhibited) and in those treated with both Lat A and DTT (both vertical migration and the xanthophyll cycle inhibited). The inhibitor solutions were added after biofilm was fully formed, in a total of 200 μL for both the Lat A and the Lat A + DTT solutions. The same volume of

252 filtered seawater was added to the control samples. The solutions were added carefully
253 to minimize biofilm disturbance, by pipetting small volumes onto the sediment surface.
254 A minimum of 30 min was given for the inhibitors to diffuse and for the biofilms to
255 stabilize before measurements were started.

256 **Inhibitor preparation and effective dosage.** Solutions of Lat A of different
257 concentrations, ranging from 5 to 15 µM, were prepared from a concentrated solution (1
258 mM) prepared from dissolving purified Lat A (Sigma-Aldrich) in dimethylsulfoxide.
259 The minimum effective dosage of Lat A to induce inhibition of vertical migration was
260 determined following Cartaxana & Serôdio (2008). Samples treated with different
261 concentrations of Lat A (final volume, 200 µL) were darkened close to the time
262 expected for tidal flood, known to induce a rapid downward migration. The degree of
263 migration inhibition was estimated from the decrease in surface biomass following
264 darkening, as estimated from dark-adapted fluorescence level, F_o. Three replicated
265 samples were tested for each Lat A concentration.

266 DTT (BDH-Prolabo) was prepared fresh as in Lavaud et al. (2002a). A stock
267 solution of 300 mM (in ethanol) was diluted in filtered seawater to prepare working
268 solutions of concentrations ranging from 3.3 to 15 mM. The minimum effective dosage
269 of DTT was determined by measuring NPQ development upon exposure to 400 µmol
270 quanta m^{-2} s^{-1} for 30 min in samples treated with increasing concentration of DTT (final
271 volume, 200 µL). Three replicated samples were tested for each DTT concentration. For
272 the light stress experiments, samples were treated with 200 µL of a combined solution
273 of Lat A and DTT, prepared using the concentration of each inhibitor determined from
274 the effective dosage tests (see Results).

275 **Taxonomic composition.** In one of the trays, microalgae were collected by
276 covering the sediment with two layers of a 100 µm-mesh. The trays were exposed to

low indirect natural light from a north facing window (< 200 µmol quanta m^{-2} s^{-1}) during the day following the sampling. The upper mesh was removed at the time of middle emersion period and it was washed with filtered (0.2 µm) natural sea water. The samples were fixed in Lugol and preserved at 4°C until their analysis. Diatom species were identified and counted using definitive mounts in Naphrax after cleaning the cells by cremation (2 h, 450°C) (Méléder et al. 2007). Taxonomic determination was performed by microscope on the basis of morphological criteria. A total of ca. 300 diatom frustules were counted to determine specific abundances.

RESULTS

Taxonomic composition

In both sampling periods, the microphytobenthic assemblages were dominated by long biraphid diatoms (length > 30 µm). In May, the assemblages were mainly dominated by *Navicula* cf. *spartinentensis* (61%, n = 350). *Staurophora salina* represented less than 20% of the assemblages but this species was two times longer than *N.* cf. *spartinentensis* (22 µm and 44 µm long, respectively). In October, the assemblages were co-dominated by *Plagiotropis seriata* (22%, n = 335) and *Staurophora salina* (19%); the size of *P. seriata* (190 µm long) was four times the one of *S. salina* one (44 µm long) strengthening its dominance in terms of biovolume. A third species, *Pleurosigma strigosum* (300 µm length) represented more than 10% of the assemblage abundance.

Photoacclimation

Significant differences were found between the light-response of ETR measured in May and October. In comparison with the ETR vs *E* curves measured in May, the ones measured in October presented significantly higher values of α (+26.7%, *t*-test, $p < 0.001$) and lower values of ETR_m (-41.5%, *t*-test, $p < 0.001$) (Fig. 1A). As a consequence, the photoacclimation parameter E_k was significantly lower in October than in May (-53.5%; *t*-test, $p < 0.001$). Regarding NPQ, significant differences were found between the light-response curves measured in the two periods (Fig. 1B). NPQ vs *E* curves measured in May reached lower levels within the range of applied irradiances (on average, 2.19 and 3.25 at 700 μmol quanta m^{-2} s^{-1}, in May and October, respectively), although the values of NPQ_m were not significantly different (*t*-test, $p = 0.425$). The light-response curves were more sigmoid in May than in October (*t*-test, $p = 0.001$), the largest differences being found regarding the light level required for induction of NPQ, indicated by the parameter E_{50}, which was significantly lower in October than in May (-38.5%; *t*-test, $p = 0.003$).

The light conditions in the region of the sampling area varied greatly between the two-week periods preceding the sampling periods, with global solar radiation reaching a daily average of 2369 J cm^{-2} in May, more than double the value observed in October, 1008 J cm^{-2}.

Inhibitor dosage

Vertical migration was strongly inhibited for most of the Lat A concentrations tested, with an inhibition level above 75% being obtained with only 5 μM (Fig. 2). The inhibitory response to the increase in Lat A concentration presented a clear saturation-like pattern, with the increase from 10 to 15 μM resulting in an increase in inhibition of

only 8.5%. Considering that 10 μM was enough to inhibit vertical migration by more than 90%, and the small increase obtained by applying the higher concentrations, solutions of 10 μM Lat A were used in all experiments.

The response of NPQ to the increase in DTT also showed a saturation-like pattern, characterized by a strong decrease for concentrations up to 5 mM, and a virtually constancy for concentrations above this value (NPQ decreased by 19% between 5 and 15 mM; Fig. 3). However, even when the highest DTT concentration was applied, NPQ was never completely eliminated, remaining above 1.0. In all further experiments, a concentration of DTT of 10 mM was used.

Light stress exposure and recovery

Figure 4 exemplifies the variation of $\Delta F/F_m'$ during a light stress-recovery experiment. On control samples, exposure to high light induced an immediate and marked decrease in $\Delta F/F_m'$ from ca. 0.63 to values slightly below 0.1 (Fig. 4). $\Delta F/F_m'$ further decreased to values close to zero during the first 15 min of exposure, after which it gradually recovered, stabilizing at values around 0.1 after 90 min and until the end of the high light period. On inhibitor-treated samples, $\Delta F/F_m'$ also decreased to values close to zero upon the start of high light exposure, but, as opposed to control samples, never showed any appreciable recovery, remaining below 0.05 (Fig. 4). However, $\Delta F/F_m'$ levels were usually higher in Lat A-treated samples than in those treated with both inhibitors (Figs. 4, 5). Following the transition to low light, a clear recovery response was observed for all samples, with $\Delta F/F_m'$ reaching in all cases over 60% of initial values after 15 min. Treatment with Lat A effectively inhibited vertical migration during the whole experiment, as indicated by the small variation in F_s in Lat A-treated

samples (on average, -12.1% for samples treated with Lat A and Lat A+DTT) as compared with the controls (-43.5%; Fig. 6). The effects of inhibitors were particularly evident during recovery under low light, during which $\Delta F/F_m'$ followed the negative exponential pattern described by Eq. (6), the fit of which was very good in all cases ($r^2 > 0.91$; Fig. 7). Control samples recovered more rapidly than those treated with inhibitors, so that after 3 min after return to low light, $\Delta F/F_m'$ of non-inhibited samples was over 70% and 60% higher than on samples treated with Lat A in May and October, respectively. In both periods these differences were gradually reduced during exposure to low light, but after 10.5 min the percentage of recovery was significantly different among treatments and sampling periods (two-way ANOVA, $p < 0.001$ for both factors). In both May and October, the recovery of $\Delta F/F_m'$ was higher in the controls than in the Lat A-treated samples (Control vs Lat A; Tukey's post-hoc test, $p = 0.043$ and $p = 0.010$, respectively), which was in turn higher than in samples treated with Lat A and DTT (Lat A vs Lat A+DTT; Tukey's post-hoc test, $p = 0.042$ and $p = 0.030$, respectively). The percentage of recovery was in all cases significantly higher in May than in October (Tukey's post-hoc test, $p < 0.05$), with the exception of samples treated with both inhibitors (Tukey's post-hoc test, $p = 0.107$).

Photoprotection efficiency and extent of photoinhibition

Depending on the species, the full recovery of the xanthophyll cycle after a transition from high to low light mainly occurs after 6 min to 15 min (Goss et al. 2006, Lepetit & Lavaud, pers. obs.). Considering the intermediate period of 10.5 min, the recovery of $\Delta F/F_m'$ at this time was used as an estimate of the photoprotection capacity and to calculate the extent of photoinhibition occurred. The results indicate that the

microphytobenthos biofilms had a large photoprotective capacity in both periods, with a correspondingly low percentage of photoinhibition below 25%, although higher in May than in October (87.7 and 78.0%; Fig. 8, Table 2). From the reduction in the photoprotection capacity measured in samples treated with inhibitors, the contribution of vertical migration and of the xanthophyll cycle to overall photoprotection were estimated to reach a combined value only slightly above 20% (Table 2). While in May the two processes had a comparable contribution to photoprotection, the relative importance of the xanthophyll cycle was reduced to 7.2% in October.

DISCUSSION

Photoacclimation and susceptibility to photoinhibition

Comparatively to May, samples collected in October appeared acclimated to lower light levels, showing the pattern typically associated to 'shade-acclimation': a combination of higher values of α and of lower values of ETR_m, resulting in lower values of E_k, usually taken as an indication of photosynthesis saturating at lower irradiances. This change in photoacclimation state between May and October was consistent with the observed seasonal change in solar light conditions preceding the two sampling periods (i.e. global solar radiation more than two times higher in May than in October). These results also generally confirmed previous observations on the seasonal variability of microphytobenthos photosynthetic performance, showing patterns of acclimation to higher light levels during spring/summer and to lower levels in autumn/winter (Blanchard et al. 1997, Migné et al. 2004, Serôdio et al. 2006). They were also

consistent with the photoacclimation response of benthic diatoms grown in culture exposed to low and high-light regimes (Perkins et al. 2006, Schumann et al. 2007, Cruz & Serôdio 2008). Increases of α, as the observed from May to October, are commonly attributed to an increase in the cellular content of light-harvesting pigments, increasing the fraction of incident light that is intercepted and absorbed for photosynthesis; decreases in ETR_m are typically associated with the decrease of the activity of the electron transport chain or the Calvin cycle, limiting factors of light-saturated photosynthesis (Henley 1993, MacIntyre et al. 2002, Behrenfeld et al. 2004).

A change in light response was also noticeable regarding NPQ, with the samples collected in October showing NPQ activation starting at lower light levels (lower E_{50}) and higher values of NPQ for most irradiances (higher NPQ_m). As with ETR, the observed variation in the NPQ vs *E* curves was consistent with the previously reported for microphytobenthos (Serôdio et al. 2006) or for benthic diatoms acclimated to different light regimes (Cruz & Serôdio 2008).

However, while changes in the light-response of ETR may be interpreted and related to underlying physiological processes in a relatively straightforward manner, the physiological meaning of changes in NPQ levels is more difficult to ascertain. This is because the two components of NPQ, q_E (photoprotection) and q_I (photoinhibition) can only be distinguished through the analysis of the recovery kinetics after exposure to high light, but not from NPQ light curves. In this study, the light stress-recovery experiments allowed to conclude that the observed change in the NPQ light-response curves was due to a decrease in the q_E component and a concomitant increase in the q_I component. In the absence of information from NPQ recovery kinetics, similar increases in NPQ vs *E* curves in autumn/winter periods have been, perhaps wrongly,

426 interpreted as being due to an increase in photoprotective capacity (Serôdio et al. 2005,
427 2006).
428 Furthermore, the results from the light stress-recovery experiments revealed an
429 association between photoacclimation status and photoprotection efficiency, not shown
430 before for these communities. Whatever the cause (see below), the acclimation to high
431 light levels in summer was associated to a high photoprotection capacity and the low
432 light-acclimation in autumn to a general loss in photoprotection and a higher
433 susceptibility to photoinhibition.
434
435 **Photoprotection vs photoinhibition**
436
437 A central finding of this study is that photoinhibition was in all cases
438 considerably low (ca. 20%), indicating photoprotection to be particularly efficient in the
439 studied microphytobenthos biofilms. Despite the general view that these assemblages
440 are largely immune to photoinhibition (Blanchard et al. 2004, Waring et al. 2007,
441 Mouget et al. 2008), this process has been shown to occur under *in situ* conditions
442 (Serôdio et al. 2008). Curiously, the rates of photoinhibition estimated in the cited
443 study, reaching up to ca. 18%, are similar to the values here reported, despite the fact
444 that they were estimated from hysteresis patterns observed during entire low tide
445 exposure periods. The results of the present study therefore confirm that the
446 photoprotective mechanisms available to benthic diatoms are not completely efficient in
447 preventing some degree of photoinhibitory damage. However, it should be stressed the
448 difficulty in comparing the measured rates of photoinhibition with results published for
449 other habitats, or for other estuarine primary producers such as phytoplankton,
450 seagrasses or macroalgae. Apart from the light history and the species-specific

differences, the extent of photoinhibition is directly related to light dosage, determined by light intensity and duration of exposure, both largely variable amongst the different experimental protocols used in different laboratory and field studies.

A number of unaccounted factors may have contributed for the measured low values of q_I. Firstly, the well-known effect of depth-integration of subsurface fluorescence (Forster & Kromkamp 2004, Serôdio 2004). This effect is caused by the fact that only the cells at or near the surface are actually exposed to measured levels of high light, and that the fluorescence signal measured at the surface also accounts for cells positioned deeper in the photic zone and exposed to lower light levels. The expected effect is a light-dependent overestimation of biofilm-level $\Delta F/F_m'$ relatively to the inherent, physiological values of the cells at the surface, which is then expected to cause a systematic overestimation of q_E and the underestimated of q_I (Serôdio 2004). However, besides this static effect, also dynamic effects can be expected. During prolonged exposure to high light, the downward migration of microalgae to less illuminated layers is likely to induce a gradual increase of $\Delta F/F_m'$ (as measured at the surface), independently of any photophysiological changes, thus causing the overestimation of q_E. It is also conceivable that these types of effects may affect the measurement of $\Delta F/F_m'$ during the recovery under low light, due to upward migration as a response to the decrease in incident irradiance. This, however, seems less likely due to the relatively short time of this period and to the fact that a transition from high to low light is a weaker stimulus for vertical migration, especially if coinciding with the end of the low tide period (Coelho et al. 2011).

A second factor that might explain the low values of q_I is the light doses applied during the light stress-recovery experiments in the laboratory. Because these (3 hrs, 1200 µmol quanta m^{-2} s^{-1}) were likely lower than the ones received during a typical

period of exposure at low tide (up to 8-10 hrs, 1500-2000 µmol quanta m^{-2} s^{-1}), larger, but still ecologically relevant, light doses could have been applied which would likely induce larger cumulative photoinhibitory effects. The light exposure conditions applied in this study, both regarding light intensity and duration, resulted from a compromise between inducing measurable effects, instrument limitations (maximum PAR irradiance provided by the imaging fluorometer) and minimizing uncontrollable experimental conditions (excessive sample heating and desiccation caused by the fluorometer LED panel). Despite these limitations, mostly instrument-related, the laboratory experimental approach used in this study has the advantage over studies carried out under *in situ* conditions (e.g. Serôdio et al. 2008; Perkins et al. 2010) of allowing applying controlled and reproducible conditions, making it possible to directly compare the migratory and physiological responses of samples collected in different places and occasions.

The estimation of q_E and q_I is also directly affected by the type of analysis made on the recovery kinetics in order to distinguish the two components of NPQ. For higher plants, q_E and q_I are distinguished on the basis of the recovery rate of F_v/F_m, typically 10-15 min, assumed to correspond to the full reversal of the xanthophyll cycle (Horton & Hague 1988, Ruban & Horton 1995). Following the common practice for the distinction of q_E and q_I, in this study these two components of NPQ were estimated based on a relaxation time of the xanthophyll cycle of 10.5 min. However, to evaluate the possible effects of considering different times for the reversal of the xanthophyll cycle on the relative magnitude of q_E and q_I, a sensitivity analysis was performed, consisting on the re-calculation of these estimates when considering 6 and 15 min, values matching the range of relaxation times of the xanthophyll cycle expectable for diatoms (Gross et al. 2006, Lepetit & Lavaud, pers. obs.). The use of these different recovery periods did not alter significantly the general findings of the study, including

high levels of recovery and low photoinhibition rates, the increase in photoinhibition levels from May to October, and a relatively low (< 30%) combined contribution of vertical migration and xanthophyll cycle to overall photoprotection (Table 2). Nonetheless, this analysis shows some effects, although largely expected from the asymptotic pattern of $\Delta F/F_m'$ recovery during the considered period: the use of a shorter period resulted in the estimation of lower rates of recovery, leading to a likely overestimation of photoinhibition rates; conversely, longer periods resulted in larger rates of recovery and probably overestimated levels of photoprotection (Table 2). Moreover, due to the different relaxation patterns of samples exposed to different treatments, the evaluation of the relative importance of vertical migration and the xanthophyll cycle was also affected by the time period considered, with shorter and longer recovery periods resulting in a higher apparent contribution of vertical migration and of the xanthophyll cycle, respectively. These effects, however, did not affect substantially the overall pattern of variation of the role of the two photoprotective processes between the two sampling periods.

Recently, more sophisticated methods, based on the mathematical modeling and deconvolution of the recovery curve, were proposed to trace the recovery of each individual component of NPQ (Roháček 2010). This method could not be applied in this study because of the particularities of the xanthophyll cycle in diatoms, which may not verify the assumptions of the method. Firstly, the lack of q_T (the state-transition quenching) in diatoms (Owens 1986, Lavaud 2007, Goss & Jakob 2010), which called for the modification of this model to a two-component NPQ. Secondly, the impossibility of using changes in F_v/F_m in biofilms as an indication of photoinhibition, as this requires the darkening of the samples, known to induce changes in F_m levels due to vertical migration. Furthermore, in benthic diatoms, dark adaptation often causes the

526 F_m level to decrease to values below F_m' levels measured under low light (Serôdio et al.
527 2006). These reasons also prevented the use of other recently proposed methods to
528 quantify the components of NPQ (Ahn et al. 2009, Guadagno et al. 2010).
529 The formation of DT in the dark and thus anoxic subsurface layers of the
530 sediment, known to occur in diatoms (Jakob et al. 2001), and especially in benthic
531 assemblages (Serôdio et al. 2006), is a likely explanation for the apparent impossibility
532 to completely eliminate NPQ by applying the xanthophyll cycle inhibitor DTT (Fig. 3).
533 The DT thus formed would remain present despite the treatment with DTT, which
534 prevents new conversion of DD to DT, but does not induce the reversed reaction. Upon
535 exposure to high light, the oxygenation of DT-rich subsurface layers would allow for
536 the observed rise in NPQ, as the formation of NPQ from DT is known to be inhibited by
537 anoxia (Cruz et al. 2011).
538
539 **Photoprotection: vertical migration vs xanthophyll cycle**
540
541 The use of specific inhibitors for vertical migration and for the operation of the
542 xanthophyll cycle allowed estimating the relative contribution of each of these
543 processes to overall photoprotection of the biofilm. The results showed a change with
544 season and photoacclimation state of their relative importance. While in May the two
545 processes seemed to contribute similarly to biofilm photoprotection, the loss of
546 photoprotection capacity from May to October was associated to a decrease in the
547 contribution of the xanthophyll cycle, so that vertical migration became the dominant
548 photoprotective process. The observed change in the species composition of the
549 microphytobenthic assemblage may explain this difference as the activity of the
550 xanthophyll cycle can differ from a species to another (Lavaud et al. 2004, Goss et al.

2006). It may be also hypothesized that this difference is related to the decrease in rates of enzymatic conversion between DD and DT associated to photoacclimation or due to acclimation to lower temperatures (Van Leuwee et al. 2008), an effect that is also species-related (Salleh & McMinn, 2011). Nevertheless, these results indicate that behavioral photoprotection seems able to maintain the overall photoprotection capacity, compensating for the decrease in the contribution of the xanthophyll cycle during the winter season.

The change in species composition, involving a dominance of larger cells in October, could also have affected the migratory response of the assemblages to high light. However, although some studies have shown a relation between migratory cell size and migratory behaviour in sediments (Hay et al. 1993, Underwood et al. 2005), there is no evidence that cell size is an important factor regarding the migratory response to light stress.

Vertical migration and the xanthophyll cycle have been considered as the main photoprotective mechanisms in microphytobenthos biofilms (Serôdio et al. 2005, Jesus et al. 2006, Mouget et al. 2008, Serôdio et al. 2008; Perkins et al. 2010). A perhaps surprising result of this study is the relative low contribution of these two processes to global photoprotection. This calls for the potential role of other processes responsible for the observed low rates of photoinhibition. Likely candidates include the cyclic electron flow around PSII (Lavaud et al. 2002b, 2007), the efficient scavenging of reactive oxygen species (Roncarati et al. 2008, Waring et al. 2010) or high turnover rates of the PSII protein D1 (Wu et al. 2011).

Use of inhibitors on microphytobenthic biofilms

An aim of this study was the introduction of a new experimental protocol to estimate photoprotection efficiency and the extent of photoinhibition in microphytobenthos biofilms. This involved the combination of: (i) the use of specific inhibitors for different photoprotective processes, applied alone and in combination with each other, allowing the estimation of the relative contribution of each process to overall photoprotection, and (ii) the use of imaging fluorometry on replicated samples in well plates, taking advantage of the self-forming nature of microphytobenthos biofilms from homogenized sediments, which allowed for adequate replication and low variability between replicates, and for the simultaneous testing of different treatments.

Some potential pitfalls exist regarding the use of inhibitors on biofilms and the interpretation of results. Firstly, it must be noted that when comparing controls (no inhibitor added) with Lat A-treated samples, it is likely that the differences in fluorescence parameters observed over time may not be attributed only to changes in cell physiological conditions but also to changes in cell composition in the upper layers of the sediment. This is because in the controls, as opposed to Lat A-treated samples, cells initially at the surface likely migrated down into layers below the photic zone, therefore changing the contribution to the fluorescence signal measured at the surface. As a consequence, any observed differences are expected to represent mainly changes at the biofilm (i.e., community)-level, and not only changes in the physiology of individual cells. This also explains the need to combine Lat A and DTT if the effect of inhibiting the xanthophyll cycle is to be evaluated in the same microalgal assemblage. By adding DTT to samples treated with Lat A, it is ensured that the same cells remain in the photic zone of the sediment and that measured changes in fluorescence are due to changes in their physiological status and not to changes in community composition. If only DTT is applied (Perkins et al. 2010), only biofilm-level effects can be evaluated, as

601 many cells will likely respond to high light by migrating downward and become
602 unobservable (Oxborough et al. 2000).
603

Acknowledgements. We thank Dr. Céline Vincent for providing solar radiation data. This study was supported by FCT – Fundação para a Ciência e a Tecnologia, through grants SFRH/BSAB/962/2009 (J. Serôdio), SFRH/BD/44860/2008 (J. Ezequiel), and project MigROS (PTDC/MAR/112473/2009), and by the CNRS – Centre National de la Recherche Scientifique (‘chercheurs invités’ program, J. Serôdio and J. Lavaud), the region Charente-Maritime/CG17 (A. Barnett Ph.D. grant), and the French consortium CPER-Littoral., . We thank two anonymous reviewers for critical comments on the manuscript.

613 LITERATURE CITED

614 Admiraal, W (1984) The ecology of estuarine sediment-inhabiting diatoms. Progr
615 Phycol Res 3:269-322

616 Ahn, TK, Avenson, TJ, Peers, G, Li, Z, Dall'Osto, L, Bassi, R, Niyogi, KK, Fleming,
617 GR (2009) Investigating energy partitioning during photosynthesis using an
618 expanded quantum yield convention. Chem Phys 357:151-158

619 Behrenfeld MJ, Prasil O, Babin M, Bruyant, F (2004) In search of a physiological basis
620 for covariations in light-limited and light-saturated photosynthesis. J Phycol
621 40:4-25

622 Blanchard GF, Guarini J-M, Dang C, Richard P (2004) Characterizing and quantifying
623 photoinhibition in intertidal microphytobenthos. J Phycol 40:692-696

624 Blanchard GF, Cariou-Le Gall V (1994) Photosynthetic characteristics of
625 microphytobenthos in Marennes-Oléron Bay, France: Preliminary results. J Exp
626 Mar Biol Ecol 182:1-14

627 Blanchard GF, Guarini JM, Gros P, Richard P (1997) Seasonal effect on the the
628 relationship between the photosynthetic capacity of intertidal microphytobenthos
629 and temperature. J Phycol 33:723-728

630 Brotas V, Risgaard-Petersen N, Ottossen L, Serôdio J, Ribeiro L, Dalsgaard T (2003) *In*
631 *situ* measurement of photosynthetic activity and respiration of intertidal benthic
632 microalgal communities undergoing vertical migration. Ophelia 57:13-26

633 Cartaxana P, Ruivo M, Hubas C, Davidson I, Serôdio J, Jesus B (2011) Physiological
634 versus behavioural photoprotection in intertidal epipelic and epipsamic benthic
635 diatom communities. J Exp Mar Biol Ecol 405:120-127

636 Cartaxana P, Serôdio J (2008) Inhibiting diatom motility: a new tool for the study of the
637 photophysiology of intertidal microphytobenthic biofilms. Limnol Oceanogr
638 Meth 6:466-476
639 Cartaxana P, Brotas V, Serôdio J (2008) Effects of two motility inhibitors on the
640 photosynthetic activity of the diatoms *Cylindrotheca closterium* and
641 *Pleurosigma angulatum*. Diatom Res 23:65-74
642 Chevalier EM, Gévaert F, Créach A (2010) In situ photosynthetic activity and
643 xanthophylls cycle development of undisturbed microphytobenthos in an
644 intertidal mudflat. J Exp Mar Biol Ecol 385:44-49
645 Coelho H, Vieira S, Serôdio J (2009) Effects of desiccation on the photosynthetic
646 activity of intertidal microphytobenthos biofilms as studied by optical methods. J
647 Exp Mar Biol Ecol 381:98-104
648 Coelho H, Vieira S, Serôdio J (2011) Endogenous versus environmental control of
649 vertical migration by intertidal benthic microalgae. Eur J Phycol 46:271-281
650 Consalvey M, Paterson DM, Underwood GJC (2004) The ups and downs of life in a
651 benthic biofilm: migration of benthic diatoms. Diatom Res 19:181-202
652 Cook PLM, Røy H (2006) Advective relief of CO 2 limitation in microphytobenthos in
653 highly productive sandy sediments. Limnol Oceanogr 51:1594-1601
654 Cruz S, Goss R, Wilhelm C, Leegood R, Horton P, Jakob T (2011) Impact of
655 chlororespiration on non-photochemical quenching of chlorophyll fluorescence
656 and on the regulation of the diadinoxanthin cycle in the diatom *Thalassiosira*
657 *pseudonana*. J Exp Bot 62:509-519
658 Cruz S, Serôdio J (2008) Relationship of rapid light curves of variable fluorescence to
659 photoacclimation and non-photochemical quenching in a benthic diatom. Aquat
660 Bot 88:256-264

661 Eilers PHC, Peeters JCH (1988) A model for the relationship between light intensity
662 and the rate of photosynthesis in phytoplankton. Ecol Model 42:199-215
663 Forster RM, Kromkamp JC (2004) Modelling the effects of chlorophyll fluorescence
664 from subsurface layers on photosynthetic efficiency measurements in
665 microphytobenthic algae. Mar Ecol Prog Ser 284:9-22
666 Genty B, Briantais J-M, Baker, NR (1989) The relationship between the quantum yield
667 of photosynthetic electron transport and quenching of chlorophyll fluorescence.
668 Biochim Biophys Acta 990:87-92
669 Goss R, Pinto AE, Wilhelm C, Richter M (2006) The importance of a highly active and
670 ΔpH-regulated diatoxanthin epoxidase for the regulation of the PS II antenna
671 function in diadinoxanthin containing algae. J Plant Physiol 163:1008-1021
672 Goss R, Jakob T (2010) Regulation and function of xanthophyll cycle-dependent
673 photoprotection in algae. Photosynth Res 106:103-122
674 Grouneva I, Jakob T, Wilhelm C, Goss, R (2008) A new multicomponent NPQ
675 mechanism in the diatom *Cyclotella meneghiniana*. Plant Cell Physiol 49:1217-
676 25
677 Guadagno CR, Virzo De Santo A, D'Ambrosio N (2010) A revised energy partitioning
678 approach to assess the yields of non-photochemical quenching components.
679 Biochim Biophys Acta 1797:525-30
680 Hay SI, Maitland TC, Paterson DM (1993) The speed of diatom migration through
681 natural and artificial substrata. Diatom Res 8:371-384
682 Henley, WJ (1993) Measurement and interpretation of photosynthetic light-response
683 curves in algae in the context of photoinhibition and diel changes. J Phycol
684 29:729-739

685 Herlory O, Guarini J-M, Richard P, Blanchard G (2004) Microstructure of
686 microphytobenthic biofilm and its spatio-temporal dynamics in an intertidal
687 mudflat (Aiguillon Bay, France). Mar Ecol Prog Ser 282:33-44

688 Horton P, Hague A (1988) Studies on the induction of chlorophyll fluorescence in
689 isolated barley protoplasts. 4. Resolution of non-photochemical quenching.
690 Biochim Biophys Acta 932:107-115

691 Jakob T, Goss R, Wilhelm, C (2001) Unusual pH-dependence of diadinoxanthin de-
692 epoxidase activation causes chlororespiratory induced accumulation of
693 diatoxanthin in the diatom *Phaeodactylum tricornutum*. J Plant Physiol158:383-
694 390

695 Jordan L, McMinn A, Thompson P (2010) Diurnal changes of photoadaptive pigments
696 in microphytobenthos. J. Mar Biol Ass UK 90:1025-1032

697 Jesus B, Perkins RG, Consalvey M, Brotas V, Paterson DM (2006) Effects of vertical
698 migrations by benthic microalgae on fluorescence measurements of
699 photophysiology. Mar Ecol Prog Ser 315:55-66

700 Kromkamp J, Barranguet C, Peene J (1998) Determination of microphytobenthos PSII
701 quantum efficiency and photosynthetic activity by means of variable chlorophyll
702 fluorescence. Mar Ecol Prog Ser 162: 45-55

703 Lavaud J, Gorkom HJV, Etienne A-L (2002b) Photosystem II electron transfer cycle
704 and chlororespiration in planktonic diatoms. Photosynth Res74:51-59

705 Lavaud J, Rousseau B, Etienne A-L (2002a) In diatoms, a transthylakoidal proton
706 gradient alone is not sufficient to induce a non-photochemical fluorescence
707 quenching. FEBS Lett 523:163-166

708 Lavaud J, Rousseau B, Etienne A-L (2004) General features of photoprotection by
709 energy dissipation in planktonic diatoms (Bacillariophyceae). J Phycol40:130-
710 137

711 Lavaud L, Kroth PG (2006) In diatoms, the transthylakoidal proton gradient regulates
712 the photoprotective non-photochemical fluorescence quenching beyond its
713 control on the xanthophyll cycle. Plant Cell Physiol 47:1010-1016

714 Lavaud, J (2007) Fast Regulation of Photosynthesis in Diatoms: Mechanisms, Evolution
715 and Ecophysiology. Funct Plant Sci Biotechnol 1:267-287

716 Lavaud J, Rousseau B, Etienne AL (2004) General features of photoprotection by
717 energy dissipation in planktonic diatoms (Bacillariophyceae). J Phycol40:130-
718 137

719 Li Z, Wakao S, Fischer BB, Niyogi KK (2009) Sensing and responding to excess light.
720 Ann Rev Plant Biol 60:239-260

721 Macintyre HL, Kana TM, Anning T, Geider RJ (2002) Photoacclimation of
722 photosynthesis irradiance response curves and photosynthetic pigments in
723 microalgae and cyanobacteria. J Phycol 38:17-38

724 Méléder V, Rincé Y, Barillé L, Gaudin P, Rosa P (2007). Spatio-temporal changes in
725 microphytobenthos assemblages in a macrotidal flat (Bourgneuf Bay, France). J
726 Phycol 43: 1177–1190

727 Migné A, Spilmont N, Davoult D (2004) In situ measurements of benthic primary
728 production during emersion: seasonal variations and annual production in the
729 Bay of Somme (eastern English Channel, France). Cont Shelf Res 24:1437-1449

730 Miles A, Sundbäck K (2000) Diel variation in microphytobenthic productivity in areas
731 of different tidal amplitude. Mar Ecol Prog Ser 205:11-22

Mouget J-L, Perkins R, Consalvey M (2008) Migration or photoacclimation to prevent high irradiance and UV-B damage in marine microphytobenthic communities. Aquat Microb Ecol 52:223-232

Müller P, Li XP, Niyogi KK (2001) Non-photochemical quenching. A response to excess light energy. Plant Physiol 125:1558-1566

Nishiyama Y, Allakhverdiev SI, Murata N (2006) A new paradigm for the action of reactive oxygen species in the photoinhibition of photosystem II. Biochim Biophys Acta 1757:742-749

Olaizola M, Yamamoto HY (1994) Short-term response of the diadinoxanthin cycle and fluorescence yield to high irradiance in Chaetoceros muelleri (Bacillariophyceae). J Phycol 30:606-612

Owens TG (1986) Light-harvesting function in the diatom *Phaeodactylum tricornutum* II. Distribution of excitation energy between the photosystems. Plant Physiol 80:732-738

Owens TG, Wold ER (1986) Light-harvesting function in the diatom *Phaeodactylum tricornutum* I. Isolation and characterization of pigment-protein complexes. Plant Physiol 80:732-738

Oxborough K, Hanlon ARM, Underwood GJC, Baker NR (2000) In vivo estimation of the photosystem II photochemical efficiency of individual microphytobenthic cells using high-resolution imaging of chlorophyll a fluorescence. Limnol Oceanogr 45:1420-1425

Perkins RG, Mouget J-L, Lefebvre S, Lavaud J (2006) Light response curve methodology and possible implications in the application of chlorophyll fluorescence to benthic diatoms. Mar Biol 149:703-712.

Perkins RG, Lavaud J, Serôdio J, Mouget, J-L, Cartaxana P, Rosa P, Barillé L, Brotas V, Jesus BM (2010) Vertical cell movement is the primary response of intertidal benthic biofilms to increasing light dose. Mar Ecol Prog Ser 416:93–103

Perkins RG, Kromkamp J, Serôdio J, Lavaud J, Jesus B, Mouget J-L, Lefebvre S, Forster R. The application of variable chlorophyll fluorescence to microphytobenthic biofilms. *In* Sugget D, Prasil O, Borowitzka MA (eds) Chlorophyll *a* Fluorescence in Aquatic Sciences: Methods and Applications, Series: Developments in Applied Phycology Vol. 4-Chapter 12, Springer, pp 237-276.

Rijstenbil, JW (2005) UV- and salinity-induced oxidative effects in the marine diatom *Cylindrotheca closterium* during simulated emersion. Mar Biol 147:1063-1073

Ritchie RJ (2008) Fitting light saturation curves measured using modulated fluorometry. Photosynth Res 96:201-15

Roháček K (2010) Method for resolution and quantification of components of the non-photochemical quenching (q_N). Photosynth Res 105:101-113

Roncarati F, Rijstenbil JW, Pistocchi R (2008) Photosynthetic performance, oxidative damage and antioxidants in Cylindrotheca closterium in response to high irradiance, UVB radiation and salinity. Mar Biol 153:965-973

Ruban, AV, Lavaud, J, Rousseau, B, Guglielmi, G, Horton, P, Etienne, AL (2004) The super-excess energy dissipation in diatom algae: comparative analysis with higher plants. Photosyn Res 82:165-175

Salleh S, McMinn A (2011) The effects of temperature on the photosynthetic parameter s and recovery of two temperate benthic microalgae, *Amphora* cf. *coffeaeformis* and *cocconeis* cf. *sublittoralis* (Bacillariophyceae). J Phycol 47:1413-1424

780 Serôdio J (2004) Analysis of variable chlorophyll fluorescence in microphytobenthos
781 assemblages: implications of the use of depth-integrated measurements. Aqua
782 Microb Ecol 36:137-152

783 Serôdio J, Cruz S, Vieira S, Brotas V (2005) Non-photochemical quenching of
784 chlorophyll fluorescence and operation of the xanthophyll cycle in estuarine
785 microphytobenthos. J Exp Mar Biol Ecol 326:157-169

786 Serôdio J, Lavaud J (2011) A model for describing the light response of the non-
787 photochemical quenching of chlorophyll fluorescence. Photosynth Res 108:61-
788 76

789 Serôdio J, Vieira S, Cruz S, Coelho H (2006) Rapid light-response curves of
790 chlorophyll fluorescence in microalgae: relationship to steady-state light curves
791 and non-photochemical quenching in benthic diatom-dominated assemblages.
792 Photosynth Res 90:29-43

793 Serôdio J, Catarino, F (1999) Fortnightly light and temperature variability on estuarine
794 intertidal sediments and implications for microphytobenthos primary
795 productivity. Aquat Ecol 33:235-241

796 Serôdio J, Vieira S, Cruz S (2008) Photosynthetic activity, photoprotection and
797 photoinhibition in intertidal microphytobenthos as studied in situ using variable
798 chlorophyll fluorescence. Cont Shelf Res 28:1363-1375

799 Underwood GJC (2002) Adaptations of tropical marine microphytobenthic assemblages
800 along a gradient of light and nutrient availability in Suva Lagoon, Fiji. Eur J
801 Phycol 37:449-462

802 Underwood GJC, Kromkamp J (1999) Primary production by phytoplankton and
803 microphytobenthos in estuaries. Adv Ecol Res 29:93-153

804 Underwood GJC, Perkins RG, Consalvey MC, Hanlon ARM, Oxborough K, Baker NR,
805 Paterson, DM (2005) Patterns in microphytobenthic primary productivity:
806 Species-specific variation in migratory rhythms and photosynthetic efficiency in
807 mixed-species biofilms. Limnol Oceanogr 50:755-767
808 Van Leeuwe MA, Brotas V, Consalvey M, Forster RM, Gillespie D, Jesus B,
809 Roggeveld J, Gieskes WWC (2008) Photoacclimation in microphytobenthos and
810 the role of xanthophyll pigments. Eur J Phycol 43:123-132
811 Walters RG, Horton P (1991) Resolution of components of non-photochemical
812 chlorophyll fluorescence quenching in barley leaves. Photosynth Res 27:121-133
813 Waring J, Baker NR, Underwood GJC (2007) Responses of estuarine intertidal
814 microphytobenthic algal assemblages to enhanced ultraviolet B radiation. Global
815 Change Biol 13:1398-1413
816 Waring J, Klenell M, Bechtold U, Underwood GJC, Baker NR (2010) Light-induced
817 responses of oxygen photoreduction, reactive oxygen species production and
818 scavenging in two diatom species. J Phycol 46:1206-1217
819 Wu H, Cockshutt AM, McCarthy A, Campbell DA (2011) Distinctive photosystem II
820 photoinactivation and protein dynamics in marine diatoms. Plant Physiol
821 156:2184-2195

822

823 Table 1. Notation

824

825 α, initial slope of the ETR vs E curve

826 a, b, c, parameters of the Eilers and Peeters (1988) model

827 DTT, dithiothreitol

828 $\Delta F/F_m'$, effective quantum yield of PSII

829 DD, diadinoxanthin

830 DT, diatoxanthin

831 DDE, diadinoxanthin de-epoxidase

832 *E*, PAR irradiance

833 E_{50}, Irradiance level corresponding to 50% of NPQ_m in a NPQ vs *E* curve

834 E_k, photoacclimation parameter of an ETR vs *E* curve

835 ETR, PSII electron transport rate

836 ETR_m, maximum ETR level in an ETR vs *E* curve

837 F_o, F_m, Minimum and maximum fluorescence of a dark-adapted sample

838 F_s, F_m', Steady state and maximum fluorescence of a light-adapted sample

839 Lat A, Latrunculin A

840 *n*, sigmoidicity coefficient of the NPQ vs *E* curve

841 NPQ, non-photochemical quenching

842 NPQ_m, maximum NPQ level in a NPQ vs *E* curve

843 PAR, photosynthetically active radiation

844 PSII, photosystem II

845 q_E, energy-dependent quenching

846 q_I, photoinhibitory quenching

847 *t*, time during recovery following light stress

848 XC, xanthophyll cycle

849

Table 2. Extent of photoinhibition and efficiency of photoprotection (%), calculated as percentage of $\Delta F/F_m'$ recovery after 10.5 min. Relative contributions of vertical migration and of the xanthophyll cycle to overall photoprotection (%), as calculated from the reduction of the $\Delta F/F_m'$ recovery in samples treated with Lat A and with Lat A and DTT, respectively, relatively to control samples. Mean and standard error of three replicates. Numbers within parenthesis indicate results obtained when considering 6 and 15 min of recovery, respectively.

	May	October
Photoinhibition	12.3 ± 0.55	22.0 ± 2.79
	(16.6, 11.7)	(33.7, 17.0)
Recovery	87.7 ± 0.55	78.0 ± 2.79
	(83.4, 88.3)	(66.3, 83.0)
Vertical migration	10.6	14.3
	(24.0, 3.6)	(17.0, 11.7)
Xanthophyll cycle	10.1	7.2
	(6.4, 13.2)	(7.3, 5.8)
Others	79.3	78.5
	(69.5, 83.2)	(75.7, 82.5)

859 Figure legends

860

861 Fig. 1. Light-response curves of ETR (A) and NPQ (B) measured in May and October
862 2010. Mean of six replicates. Vertical bars: one standard error. Numbers represent the
863 mean values of model parameters estimated for light-response curves measured for each
864 individual sample.

865

866 Fig. 2. Variation of migration inhibition with the concentration of added Lat A solution.
867 Mean of three replicates. Vertical bars: one standard error. Line represents the fit of
868 exponential decay model.

869

870 Fig. 3. Inhibition of NPQ as a function of concentration of added DTT solution. NPQ
871 induced upon exposure to 400 µmol quanta m^{-2} s^{-1}. Mean of three replicates. Vertical
872 bars: one standard error. Line represents the fit of exponential decay model.

873

874 Fig. 4. Light stress-recovery experiment. Variation of PSII quantum yield, $\Delta F/F_m'$,
875 during sequential exposure to low light (pre-stress, 55 µmol quanta m^{-2} s^{-1}), light stress
876 under high light (high light, 1200 µmol quanta m^{-2} s^{-1}, 180 min) and recovery under low
877 light (recovery, 55 µmol quanta m^{-2} s^{-1}, 10.5 min) for controls and for samples treated
878 with migration inhibitor Lat A and with migration and xanthophyll cycle inhibitors (Lat
879 A + DTT), collected in May 2010. Mean of three replicates. Vertical bars: one standard
880 error.

881

882 Fig. 5. Images of PSII quantum yield, $\Delta F/F_m'$ (false color scale), as measured in the
883 sediment samples used in the light stress experiment described in Fig. 4 at the end of

884 first low light exposure (pre-stress, 55 µmol quanta m^{-2} s^{-1}), at the end of high light
885 exposure (high light, 1200 µmol quanta m^{-2} s^{-1}, 180 min) and following recovery under
886 low light (recovery, 55 µmol quanta m^{-2} s^{-1}, 10.5 min). Three replicated areas of interest
887 for each treatment.
888
889 Fig. 6. Images of fluorescence level F_s (false color scale) as measured in the sediment
890 samples used in the light stress experiment described in Fig. 4. at the end of first low
891 light exposure (pre-stress, 55 µmol quanta m^{-2} s^{-1}), and after recovery following end of
892 high light exposure (high light, 1200 µmol quanta m^{-2} s^{-1}, 180 min; recovery, 55 µmol
893 quanta m^{-2} s^{-1}, 10.5 min). Three replicated areas of interest for each treatment.
894
895 Fig. 7. Recovery of PSII quantum yield, $\Delta F/F_m'$, during relaxation following light stress
896 for control samples and for samples treated with migration inhibitor Lat A and with
897 migration and xanthophyll cycle inhibitors (Lat A + DTT). Lines represent the
898 exponential model described by Eq. (6) fitted to average $\Delta F/F_m'$ values. Detail of Fig. 4.
899
900 Fig. 8. Efficiency of photoprotection, as percentage of recovery after 10.5 min low light
901 following high light exposure, in May and October, for controls and inhibitor-treated
902 samples. Mean of three replicates. Vertical bars: one standard error.
903

904 Figure 1

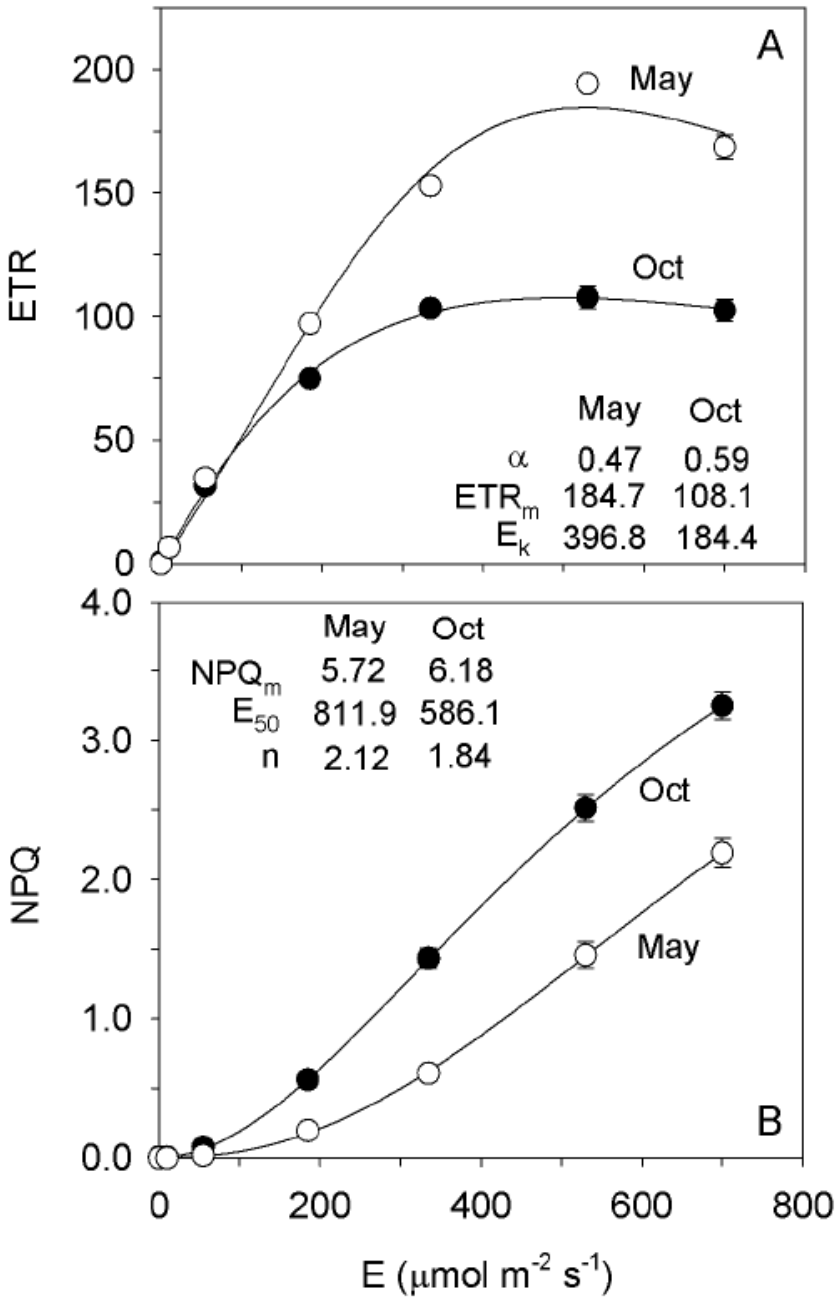

905

906

907 Figure 2

908

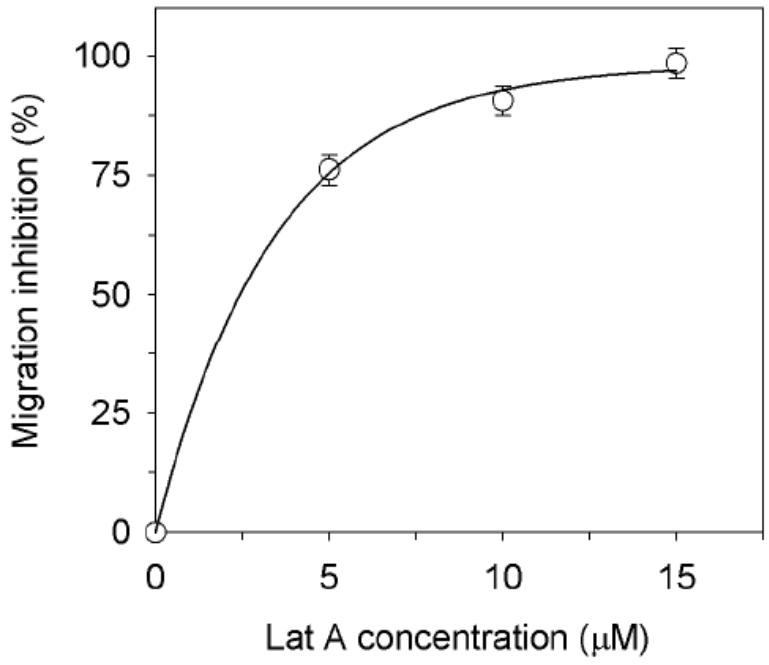

909

910

911 Figure 3

912

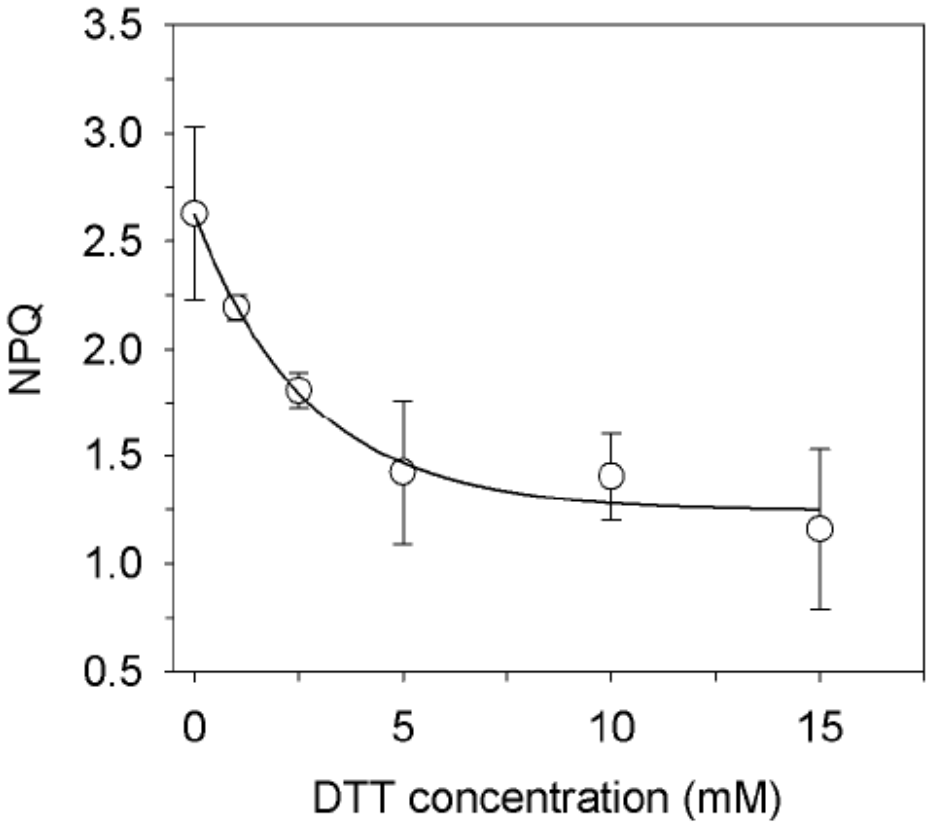

913

914

915 Figure 4

916

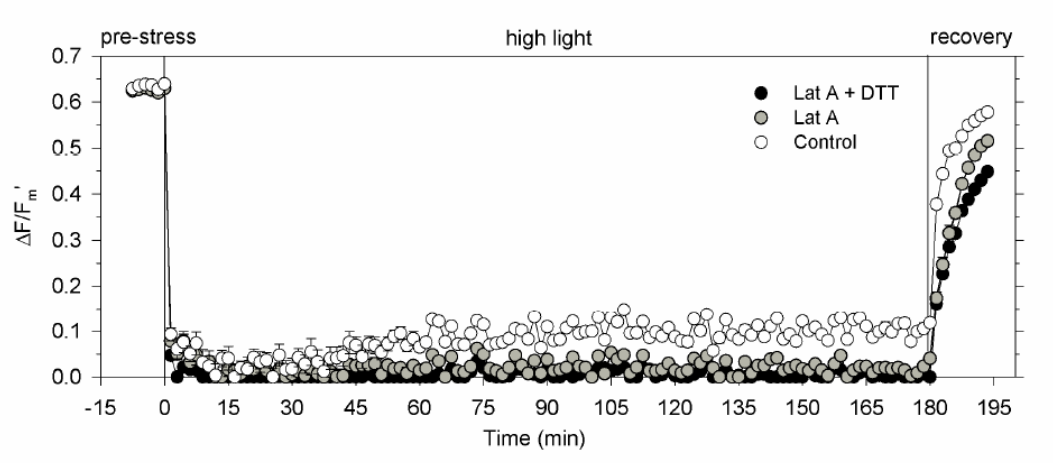

917

918

919 Figure 5

920

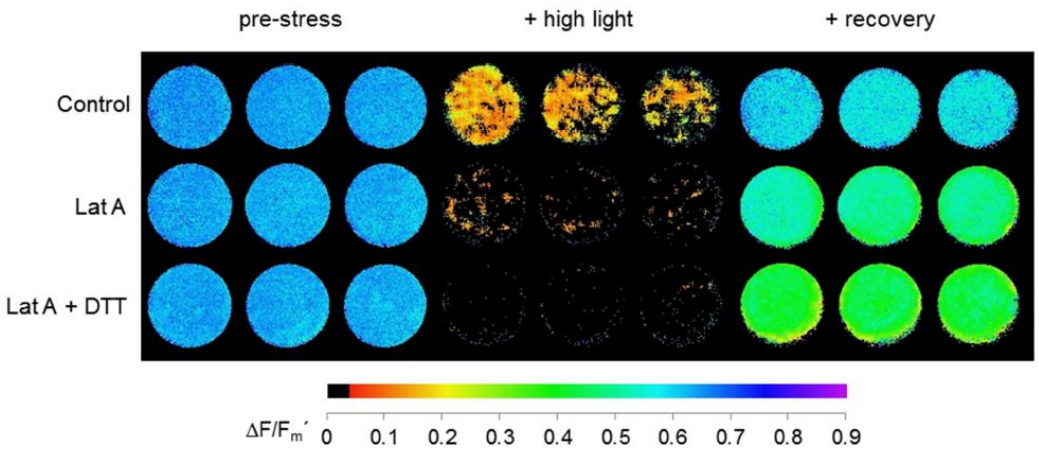

921

922

923 Figure 6

924

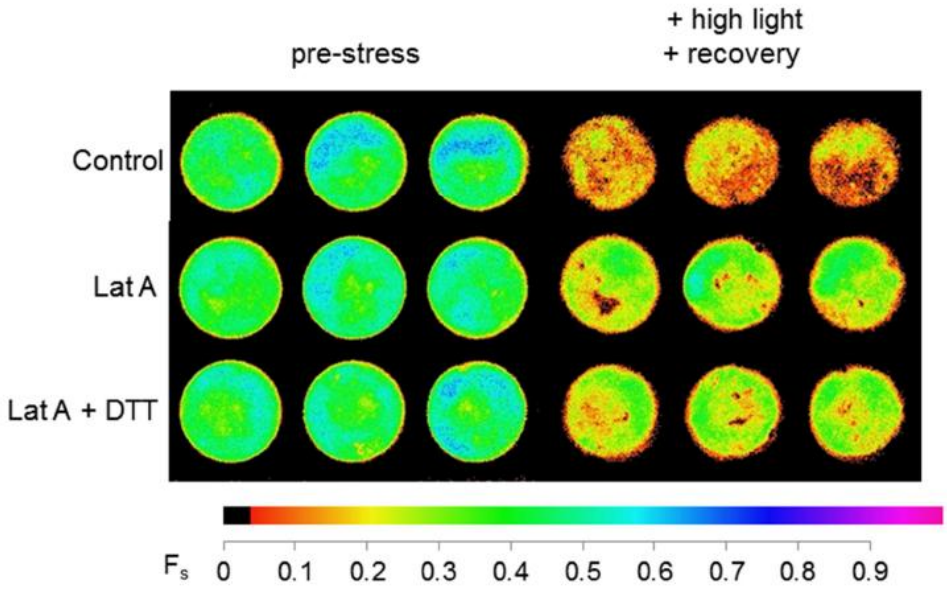

925

926

927 Figure 7

928

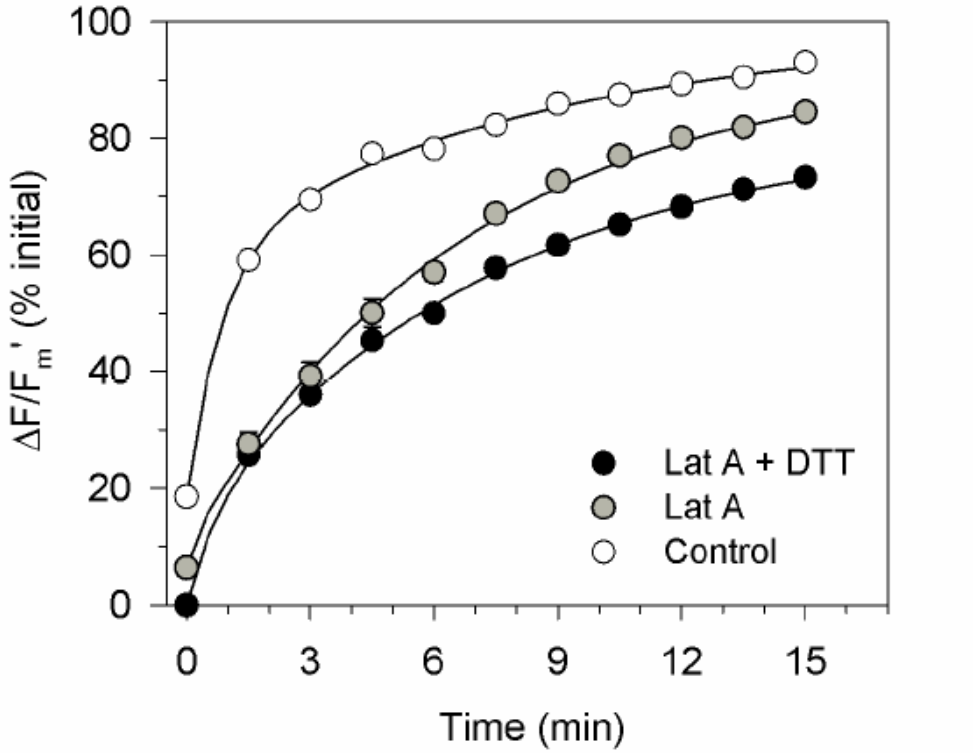

929

930

931 Figure 8

932

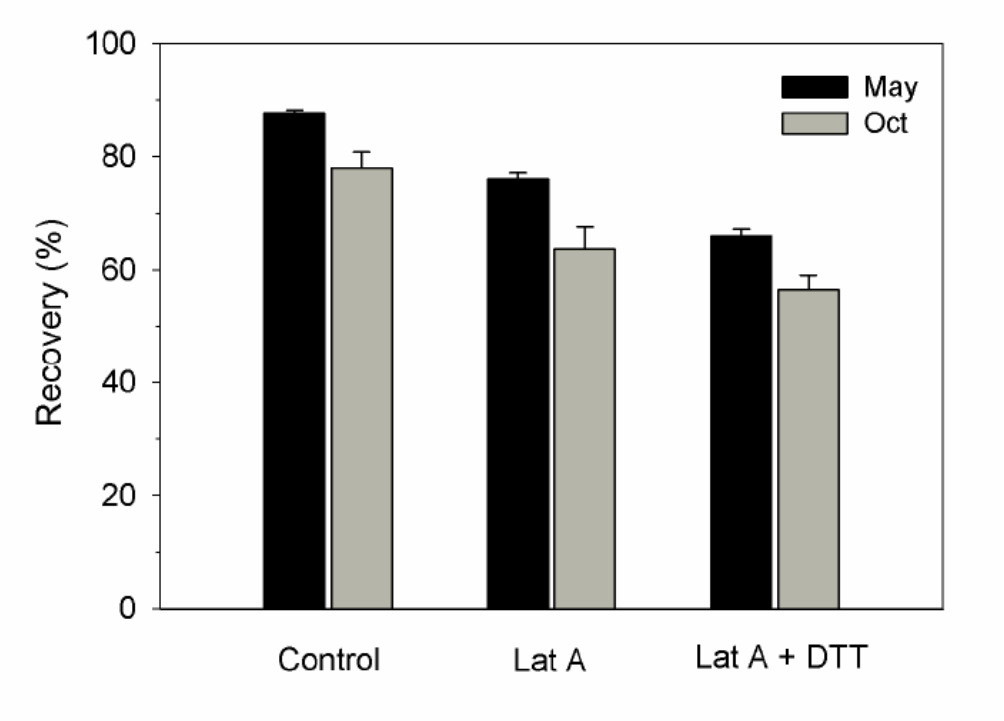

933